AGU PUBLICATIONS

Geophysical Research Letters

RESEARCH LETTER
10.1002/2015GL063557

Key Points:
- Natural variability dominates the recent ENSO-monsoon relationship change
- Forced rainfall change may weaken the ENSO-monsoon relation in the future
- CMIP5 models show large intermodel spread

Supporting Information:
- Text S1, Figures S1–S3, and Table S1

Correspondence to:
X. Li,
xqli@ldeo.columbia.edu

Citation:
Li, X., and M. Ting (2015), Recent and future changes in the Asian monsoon-ENSO relationship: Natural or forced?, *Geophys. Res. Lett.*, *42*, doi:10.1002/2015GL063557.

Received 19 FEB 2015
Accepted 1 APR 2015
Accepted article online 7 APR 2015

Recent and future changes in the Asian monsoon-ENSO relationship: Natural or forced?

Xiaoqiong Li[1,2] and Mingfang Ting[1]

[1]Lamont-Doherty Earth Observatory, Columbia University, Palisades, New York, USA, [2]Department of Earth and Environmental Sciences, Columbia University, New York, New York, USA

Abstract The Asian monsoon-ENSO (El Niño–Southern Oscillation) relationship in the 20th and 21st centuries is examined using observations and Coupled Model Intercomparison Project Phase 5 (CMIP5) model simulations. CMIP5 models can simulate the ENSO-monsoon spatial structure reasonably well when using the multimodel mean. Running correlations show prominent decadal variability of the ENSO-monsoon relationship in observations. The modeled ENSO-monsoon relation shows large intermodel spread, indicating large variations across the model ensemble. The anthropogenically forced component of ENSO-monsoon relationship is separated from the naturally varying component based on a signal-to-noise maximizing empirical orthogonal function analysis using global sea surface temperature (SST). Results show that natural variability plays a dominant role in the varied ENSO-monsoon relationship during the 20th century. In the 21st century, the forced component is dominated by enhanced monsoon rainfall associated with SST warming, which may contribute to a slightly weakened ENSO-monsoon relation in the future.

1. Introduction

The Asian monsoon variability and change have attracted tremendous attention in the climate research community [e.g., *Kumar et al.*, 2006; *Turner and Annamalai*, 2012; *Wang et al.*, 2014] due to the system's serious impacts on the region's socioeconomic development [e.g., *Kumar et al.*, 2004; *Mirza*, 2011]. On interannual time scale, the Asian summer monsoon variability is strongly associated with the El Niño–Southern Oscillation (ENSO), as suggested by the abundance of observational, modeling, and paleoclimate studies [e.g., *Kumar et al.*, 2006; *Cook et al.*, 2010; *Mishra et al.*, 2012]. During a warm ENSO event with anomalously high sea surface temperature (SST) over the eastern tropical Pacific, convection in the western Pacific shifts to the central and eastern Pacific, which then suppresses the convection in the Asian monsoon region as well as the western Pacific warm pool region, resulting in monsoon failure [e.g., *Rasmusson and Carpenter*, 1983; *Ropelewski and Halpert*, 1987; *Webster and Yang*, 1992; *Lau and Nath*, 2000; *Wang et al.*, 2003].

Recent observational analyses, however, suggest that the ENSO-monsoon relationship may have weakened or broken down for the recent decades [*Kumar et al.*, 1999; *Kinter et al.*, 2002]. Some studies suggest it is likely that anthropogenic global warming may have been the cause of the weakening relationship. *Kumar et al.* [1999] examined observed data and proposed two possible reasons for the changing ENSO-monsoon relation due to global warming: first, the southeastward shift of the climatological Walker Circulation due to greenhouse warming disconnects the Indian monsoon from the region of ENSO impact; second, the increased winter and spring surface temperature and reduced snow cover over Eurasia due to greenhouse warming enhances land-sea thermal contrast and favors a stronger monsoon, thus reduces the negative impact of El Niño on monsoon rainfall. *Ashrit et al.* [2001], based on a single realization of the Max-Plank Institute climate model, confirmed that the increase in ground temperature over Eurasian continent due to greenhouse warming led to a stronger monsoon and thus a reduced impact from ENSO. Thus, there are indications in both models and observations that a weakening of the ENSO-monsoon relationship could occur in a warmer future climate. On the contrary, several studies suggest that this weakening relationship is more likely due to natural climatic variability rather than a response to global warming [e.g., *Kripalani et al.*, 2003; *Kitoh*, 2007]. Using multiple model simulations for the Intergovernmental Panel on Climate Change (IPCC) Fourth Assessment Report (AR4) for the 20th century and global warming experiments in which the atmospheric CO_2 concentration was raised to twice the preindustrial value, *Annamalai et al.* [2007] showed that the ENSO-monsoon correlation in the warming runs is very similar to that in the historical simulations, countering the argument that the connection will weaken as climate warms.

It is noted that the ENSO-monsoon system has undergone significant interdecadal changes in observations [*Torrence and Webster*, 1999], paleoclimate reconstructions [*Berkelhammer et al.*, 2014], and long-term control simulations of coupled general circulation models (GCMs) [*Kitoh*, 2007; *Hunt*, 2014]. *Krishnamurthy and Goswami* [2000] proposed the hypothesis that the interdecadal variations of the Indian summer monsoon and tropical SST are part of a tropical ocean-atmosphere coupled mode. *Chowdary et al.* [2012] suggest that the interdecadal variations of ENSO teleconnections over the Indo-western Pacific is mainly governed by ENSO variance itself. Several studies have proposed possible mechanisms linking the decadal change of the ENSO-monsoon system to other large-scale climate variability. For example, *Kinter et al.* [2002] related the change to north Pacific SST and atmospheric circulation. *Krishnamurthy and Krishnamurthy* [2014] showed that the Pacific Decadal Oscillation (PDO) can enhance (counteract) the ENSO-monsoon relation when ENSO and PDO are in (out of) phase. *Chang et al.* [2001] suggest that the weakening ENSO-monsoon relation is most likely due to the strengthening and poleward shift of the jet stream over the North Atlantic. Using a coupled GCM, *Chen et al.* [2010] found that the Atlantic Multidecadal Oscillation (AMO) could induce coupled feedbacks in the tropical Pacific and modulate the multidecadal variation of the ENSO-monsoon connection. Some studies also address the influence of statistical stochasticism in analyzing the relationship between ENSO and monsoon rainfall [*Hunt*, 2014]. *Gershunov et al.* [2001] point out that running correlations between pairs of stochastic time series are typically characterized by low-frequency evolution; thus, the decadal fluctuations in the observed ENSO-monsoon relationship can be explained by sampling variability alone.

The ENSO signal has long been regarded as an important seasonal predictor for monsoon rainfall [e.g., *Webster and Yang*, 1992; *Ju and Slingo*, 1995]. Thus, understanding how the ENSO-monsoon relationship might change on longer time scales has strong implications to successful monsoon forecasts. In particular, it is vital to understand whether the recent weakening of the ENSO-monsoon relationship is related to anthropogenic climate change, and if so, how one would expect it to change in the future. The lack of consensus in previous studies reveals substantial uncertainties in observations and model simulations, as well as analysis methods. Many questions remain to be addressed, such as the robustness of the change in ENSO-monsoon relationship in different models and how the anthropogenically forced component can be separated from the naturally varying ENSO-monsoon relationship.

We examined the ENSO-monsoon relationship for the 20th and 21st centuries using observations and the World Climate Research Programme (WCRP) Coupled Model Intercomparison Project Phase 5 (CMIP5) model simulations. We address the following question in this paper: What are the forced and natural patterns of the ENSO-monsoon teleconnection and how is this relationship changing in the future? The paper is organized as follows. Section 2 describes observational data sets and model simulations used in the study, as well as analysis methodology. Section 3 presents results regarding the natural and forced SST-monsoon relationship. The main conclusions are summarized in section 4.

2. Data and Methods

For observed precipitation, we used monthly data from the Climate Research Unit (CRU) at the University of East Anglia version 3.2 [*Harris et al.*, 2014]. The spatial resolution is $0.5^\circ \times 0.5^\circ$, interpolated to $1^\circ \times 1^\circ$ to allow for a higher rain gauge count within each grid box. Only the grid boxes where at least one rain gauge existed in any month of the June-August (JJA) season for at least 80 years during the 1901–2005 period were used in the analysis in order to improve the data reliability. We used observed monthly SST from the National Oceanic and Atmospheric Administration (NOAA) National Climate Data Center Extended Reconstructed Sea Surface Temperatures (ERSST) version 3b [*Smith et al.*, 2008] and winds from the 20th Century Reanalysis (20CR) Project version 2 [*Compo et al.*, 2011], both with a $2^\circ \times 2^\circ$ spatial resolution.

Model simulations in this study include a multimodel ensemble of CMIP5 models [*Taylor et al.*, 2012] used in IPCC AR5. We used monthly output of 34 models for preindustrial control simulations, as well as all realizations for historical simulations and future projections under the high-end representative concentration pathway 8.5 (RCP8.5) emission scenario. Altogether 103 realizations were analyzed for the historical period and 71 for RCP8.5 (see Table S1 in the supporting information). All model outputs were interpolated to a $1^\circ \times 1^\circ$ spatial resolution for precipitation and $2^\circ \times 2^\circ$ for SST and winds.

In order to separate the naturally varying ENSO-monsoon relation and the forced response of rainfall to SST warming, we applied signal-to-noise (S/N) maximizing empirical orthogonal function (EOF) analysis [*Allen and Smith*, 1997; *Venzke et al.*, 1999; *Chang et al.*, 2000] to JJA seasonal averaged global SST of the CMIP5

multimodel ensemble to extract the externally forced signal, as in *Ting et al.* [2009, 2011]. Given the multimodel, multirealization ensemble, the total covariance matrix of the ensemble mean can be assumed as a sum of two linearly independent matrices, one for forced signal and one for internal variability (climate noise). We first determined the spatial structure of the internal modes of variability through an EOF analysis on the noise matrix, formed using the second century of the simulated SST in the preindustrial control run for each of the corresponding CMIP5 model in the analysis. These noise EOFs (retaining 80% of the total variance) were used to form a spatial prewhitening transformation matrix to filter the internal variability that was not removed by the multimodel ensemble averaging, so that the spatial covariance in the ensemble average is largely due to forced change. The leading EOF mode of the ensemble mean gives the dominant forced signal (see supporting information). We used the leading principle component (S/N PC1) as the forced index. For observations and each realization of model simulations, we regressed JJA seasonal average SST anomalies (SST_{total}) onto S/N PC1 to obtain the forced component:

$$k(x,y) = r(x,y)\frac{\sigma_{SST_{total}(x,y,t)}}{\sigma_{PC1(t)}}, \tag{1}$$

$$SST_{forced}(x,y,t) = k(x,y)\cdot PC1(t), \tag{2}$$

where $r(x,y)$ is the correlation coefficient between grid point SST and S/N PC1 and σ the corresponding standard deviation. We calculated the difference between SST_{total} and SST_{forced} to obtain the natural component ($SST_{natural}$):

$$SST_{natural}(x,y,t) = SST_{total}(x,y,t) - SST_{forced}(x,y,t), \tag{3}$$

as in *Ting et al.* [2009, 2011]; *Kelley et al.* [2012]. We then averaged SST_{total}, $SST_{natural}$ and SST_{forced} over the Niño 3.4 box (5°S–5°N, 170°W–120°W) [*Trenberth*, 1997] to obtain the total, natural and forced Niño 3.4 SST indices, respectively. The forced Niño 3.4 SST index for each CMIP5 model (using the first realization) and ERSST, as well as the total and natural Niño 3.4 SST indices for ERSST are provided in the supporting information.

3. Results

We first examined the spatial structure of the ENSO-monsoon relationship in observations and CMIP5 models. Figure 1 shows regressions of JJA seasonal average monsoon rainfall and global SST onto the total Niño 3.4 SST index for observations (Figures 1a and 1b), CMIP5 historical simulations (Figures 1c and 1d) for 1901–2005, and future projections under the RCP8.5 scenario for 2006–2099 (Figures 1e and 1f). The CMIP5 results (Figures 1c–1f) are the multimodel mean (MMM) patterns of the regression coefficients. In calculating the MMM, we first computed each model's ensemble mean regression pattern and then performed multimodel ensemble average using each model's ensemble mean. The observed (Figure 1a) and modeled (Figure 1c) rainfall patterns both show the expected strong inverse relationship with ENSO over the Indian subcontinent. The robustness is indicated by the statistical significance in Figure 1a and the high degree of model agreement in Figure 1c. The CMIP5 MMM captures the ENSO signal in monsoon rainfall variability reasonably well. The global SST regressions show the canonical ENSO patterns in both the observation (Figure 1b) and the CMIP5 MMM (Figure 1d). The ENSO-related SST anomaly in the CMIP5 MMM extends farther west compared to the observed pattern. This has been noted in previous studies to be a systematic bias of CMIP5 models, driven by unrealistic westward displacement and overestimation of the equatorial wind stress in the western Pacific [*Taschetto et al.*, 2014]. For RCP8.5, the rainfall pattern (Figure 1e) exhibits clearly weakened ENSO-monsoon connection with low model agreement in the Indian subcontinent. The SST pattern (Figure 1f) displays mixed signals of both ENSO and global warming trend. Thus, the change in rainfall pattern in Figure 1e may be a combination of natural variability and anthropogenic forcing.

To illustrate the temporal evolution of the ENSO-monsoon relation, we computed running correlations with a 31 year sliding window between the total Niño 3.4 SST index and the all-India average rainfall (weighted area average of 5°N–30°N, 70°E–90°E), for the JJA season. We used the second century of preindustrial control runs for the 34 models to examine the natural fluctuations without any external forcing, as shown in Figure 2a. The correlation values are plotted against the midpoint years of the 31 year window and box-whiskers of the

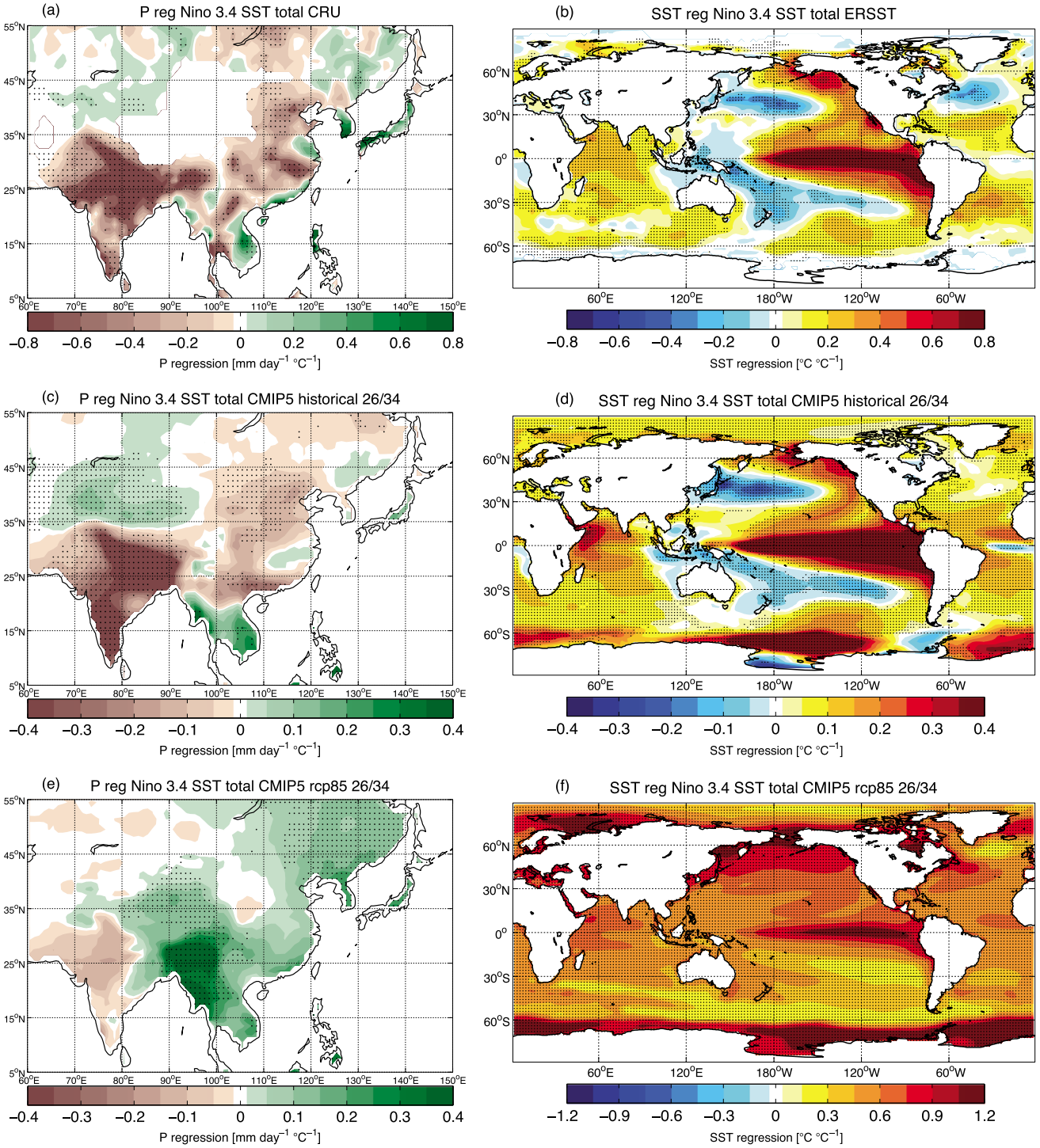

Figure 1. Regressions of JJA (a, c, e) precipitation and (b, d, f) global SST onto total Niño 3.4 SST index for (a, b) observations (CRU, ERSST) 1901–2005, (c, d) CMIP5 34 model MMM historical 1901–2005, and (e, f) RCP8.5 2006–2099 simulations. For observed precipitation (Figure 1a), only the grid boxes where at least one rain gauge existed in any month of the JJA season for at least 80 years are plotted. Stippling denotes 5% significance based on two-sided Student's *t* test in Figures 1a and 1b and 26/34 model agreement in Figures 1c–1f. Units are in mm day^{-1} °C^{-1} for Figures 1a, 1c, and 1e, and °C °C^{-1} for Figures 1b, 1d, and 1f.

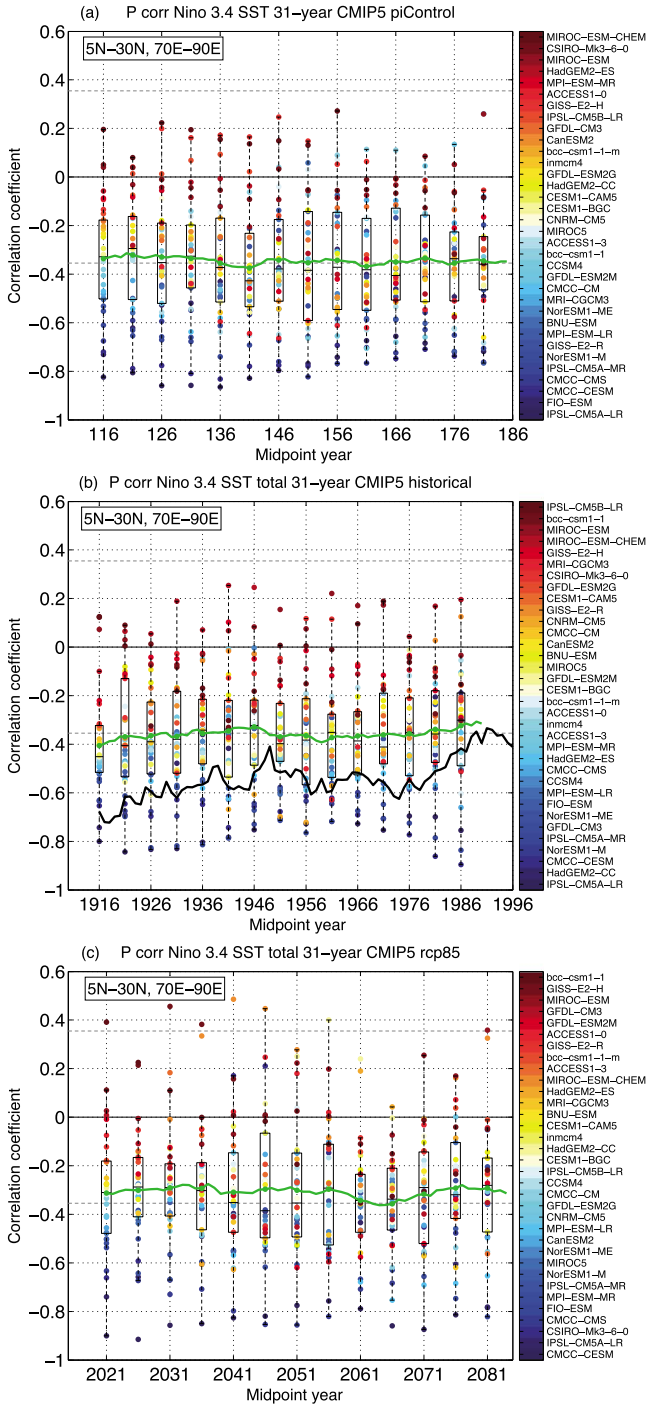

Figure 2. A 31 year running correlation between JJA India area averaged precipitation (5°N–30°N, 70°E–90°E) and total Niño 3.4 SST index plotted against the midpoint years for CMIP5 (a) preindustrial control runs, (b) historical and (c) rcp8.5, using the first realization for each model. The colored dots are correlation coefficients for individual models, plotted every 5 years. Models are ranked and assigned colors based on the correlation values for the first 31 year period. The box edges give the 25th to 75th percentiles, the whiskers extend from each end of the box to the maximum values within 1.5 times the interquartile range, and the black line in each box shows the median. Green thick lines show CMIP5 MMMs, black thick line in Figure 2b shows the result of observations using CRU and ERSST. Dashed lines denote 5% significance based on two-sided Student's *t* test.

model spread are plotted every 5 years. The box edges give the 25th to 75th percentiles, and the whiskers extend from each end of the box to the maximum values within 1.5 times ($w = 1.5$) of the interquartile range, which corresponds to approximately ± 2.7 standard deviation and 99.3% coverage if the data were normally distributed. The correlation coefficients of each model are plotted in colored dots. We ranked the models based on the correlation values for the first 31 year period and assigned each model a corresponding color. The green line shows the MMM. The corresponding results for the historical and RCP8.5 simulations are shown in Figures 2b and 2c, using the first realization for each model. The black thick line in Figure 2b is the observed 31 year running correlation based on ERSST and CRU precipitation, for a slightly extended period to 2011.

The observed ENSO-monsoon relationship in Figure 2b shows a weakening trend since the 1970s, with a ~0.25 maximum decrease in correlation value from below −0.6 to slightly above −0.4. However, there are prominent decadal fluctuations throughout the twentieth century, with a range of ~0.35 in correlation value. The first half of the century shows a similar weakening trend with a maximum decrease (~0.3) slightly exceeding the recent period. Additionally, the correlation trend reversed after 1990, suggesting a possible strengthening of the correlation in the most recent years. A significance test using the method in *Gershunov et al.* [2001] shows that the variation of the running correlation in observations during the twentieth century is not significantly different from what one would expect for correlated Gaussian noise processes at the 5% level. Thus, one cannot rule out the possibility that stochastic noise may contribute to a low-frequency correlation change as large as in observations. Comparing to model-simulated results, the observed fluctuations in correlation in Figure 2b is within the spread of the CMIP5 historical runs as well as the preindustrial simulations (Figure 2a). The modeled ENSO-monsoon relation ranges from weakly positive to highly negative values, while the MMMs in preindustrial and historical simulations are both significantly weaker than that for observations. This implies that although the MMM is able to capture the spatial pattern of the ENSO-monsoon connection (Figures 1a and 1c), there are large uncertainties within the model ensemble in the magnitude and, in some cases, even sign of the ENSO-monsoon relationship. The correlation values for individual models (colored dots) show that the spread comes from discrepancy from model to model rather than fluctuations within any single model, as the group of models with higher (lower) correlations remains rather consistent with time. In other words, models with higher correlation values tend to remain high throughout the century and vice versa. The MMM of historical simulations (Figure 2b) has little change compared to the preindustrial runs (Figure 2a). In the RCP8.5 case (Figure 2c), the MMM shows a slightly decreased correlation, dropping below the statistical significance value denoted by the dashed line.

Figure 2 suggests that anthropogenic forcing has a minor effect in the RCP8.5 case with strong anthropogenic warming, but contributes little to the ENSO-monsoon relation in the historical period. Thus, the weakening ENSO-monsoon relation in the recent decades is more likely due to decadal variability rather than the global warming trend. It is possible that greenhouse warming could contribute to a slight weakening of the ENSO-monsoon relationship in the future. However, internal variability tends to dominate, and there is substantial uncertainty with low agreement among the models. Comparing our results to earlier studies, *Ashrit et al.* [2005] showed a much stronger weakening of the ENSO-monsoon relation in the 21st century, particularly after 2050. *Ashrit et al.* [2003], on the other hand, reported no systematic change of the ENSO-monsoon relation due to greenhouse warming. These diverse results also indicate a high degree of uncertainty possibly due to model discrepancies in terms of ENSO-monsoon simulations [*Annamalai et al.*, 2007].

To separate the natural and forced ENSO-monsoon components, we applied regression analysis onto the natural and forced Niño 3.4 SST indices. Figure 3 shows the rainfall (Figures 3a, 3c, and 3e) and global SST (Figures 3b, 3d, and 3f) regression fields associated with the natural Niño 3.4 SST index for observations (Figures 3a and 3b), CMIP5 historical (Figures 3c and 3d) and RCP8.5 (Figures 3e and 3f). Both the observed (Figure 3a) and CMIP5 historical rainfall regressions (Figure 3c) are very similar to that for the total Niño 3.4 index in Figures 1a and 1c, indicating that natural variability plays the dominant role in the varied ENSO-monsoon relationship during the twentieth century. The natural component of the SST regressions (Figures 3b and 3d) are also similar to the total fields (Figures 1b and 1d), with weaker positive correlations over regions such as western tropical Pacific, tropical and northern Atlantic, and the Southern Ocean. The natural components of the regression patterns for RCP8.5 (Figures 3e and 3f), on the other hand, show distinctively different features from the total regressions (Figures 1e and 1f). The rainfall pattern (Figure 3e) gives a clear negative ENSO signal over India and is remarkably similar to the historical case (Figure 3c). The SST regression (Figure 3f) displays the typical ENSO pattern almost undistinguishable from the historical SST regression in Figure 3d and significantly different from that in Figure 1f when the forced component is included. The high

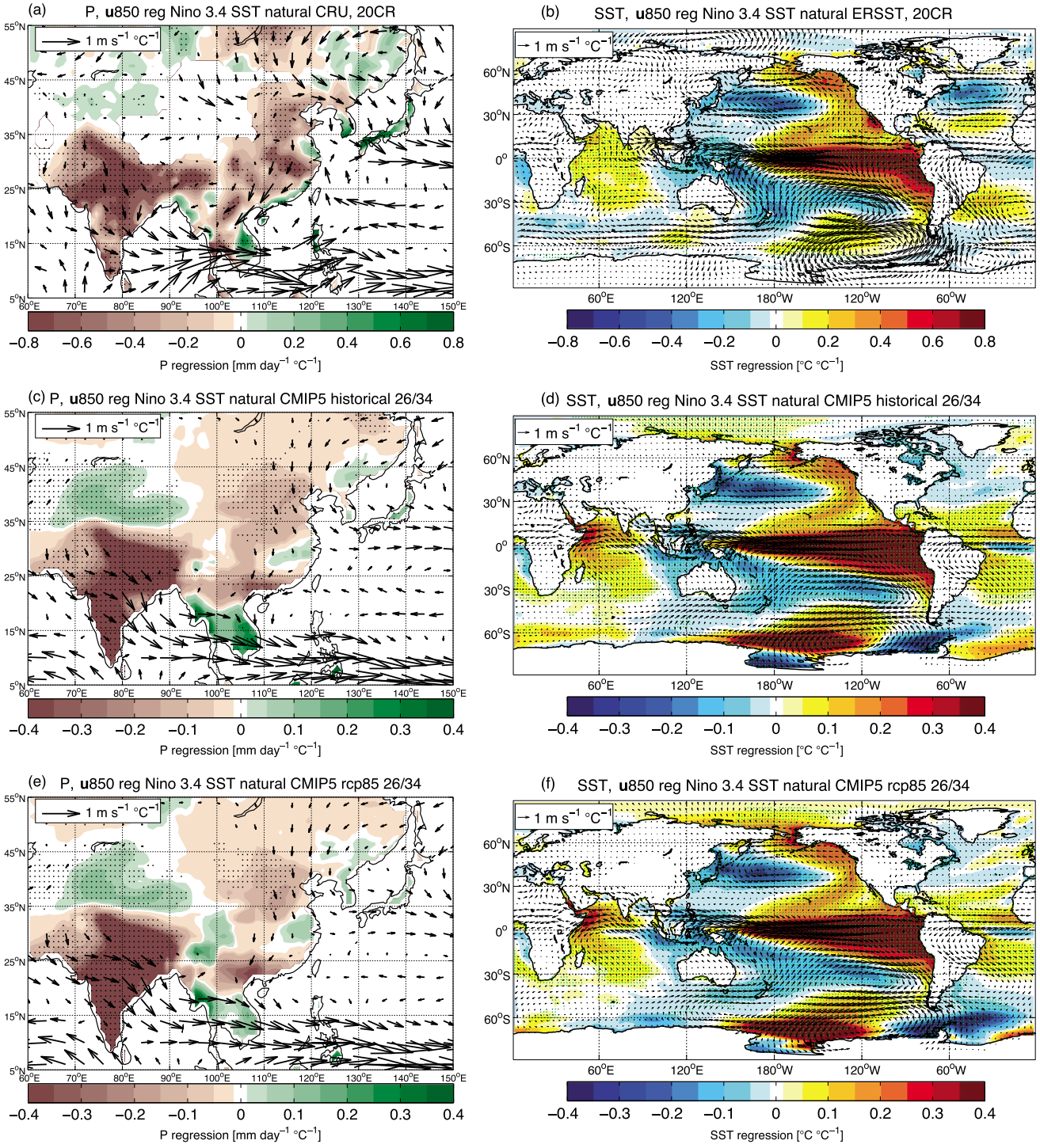

Figure 3. Shading and stippling as in Figure 1, but using natural Niño 3.4 SST index. Arrows show regressions of 850 hPa winds onto natural Niño 3.4 SST index; units are m s^{-1} °C^{-1}.

degree of similarity between Figures 3c and 3e and between Figures 3d and 3f indicates that the unforced ENSO-monsoon relationship as simulated in CMIP5 MMM is insensitive to the external radiative forcing. In all three cases, the 850 hPa wind regressions (arrows) show westerly anomalies in the western Pacific, indicating that there is a shift of the Walker circulation toward the central Pacific and the Asian monsoon is part of that shift. In the northern Indian Ocean, there are easterly wind anomalies that oppose the climatological monsoon circulation. This anticyclonic feature over the Arabian Sea and the surrounding land areas has been

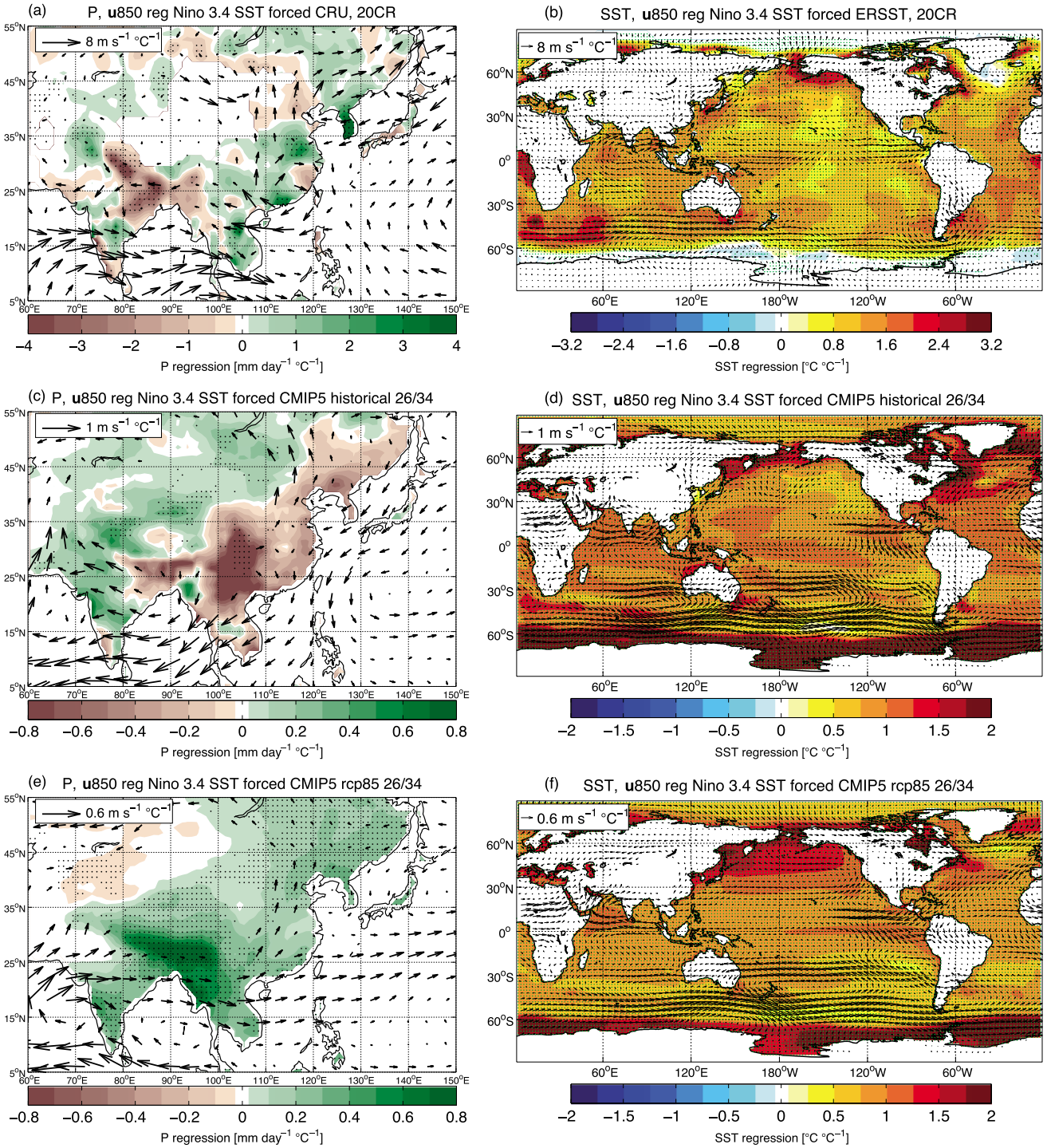

Figure 4. As in Figure 3, but using forced Niño 3.4 SST index.

addressed in *Lau and Nath* [2000] and *Lau and Wang* [2006] to be associated with the anomalous diabatic cooling in the western tropical Pacific during El Niño events. These circulation changes are consistent with the reduced monsoon rainfall during a warm ENSO phase.

The forced SST-monsoon relationship can be seen from the rainfall regressions to the forced Niño 3.4 SST time series (see supporting information), as shown in Figure 4 for observations (Figure 4a), CMIP5 historical (Figure 4b), and RCP8.5 (Figure 4c). The global SST regression to the forced Niño3.4 index is clearly a global

warming pattern in all three cases (Figures 4b, 4d, and 4f), consistent with the S/N EOF pattern (see supporting information). The corresponding rainfall regression pattern associated with the forced SST for the observation (Figure 4a) displays a drying trend in the southwest and northeast and wetting over central India. The CMIP5 historical (Figure 4c) shares some similarity with the observed pattern in India, in sharp contrast to that in east China, where the observed and modeled patterns are opposite to each other. Note that both the statistical significance in Figure 4a and the model agreement in Figure 4c are relatively low, indicating a high degree of uncertainty for the forced response in the historical period. The RCP8.5 (Figure 4e) gives a clearly enhanced rainfall trend across the Asian monsoon domain, with relatively high model agreement for most of Asia. The wetting signal associated with SST warming in the RCP8.5 scenario has contributed to the weakening of the negative Indian monsoon pattern in the 21st century (Figure 1e), given the fact that the natural component associated with ENSO generally remains unchanged (Figure 3e). The enhanced monsoon rainfall associated with forced SST is consistent with *Li et al.* [2015], who extracted the radiatively forced monsoon rainfall signal directly using the S/N EOF analysis on rainfall rather than SST. Based on moisture budget analysis, *Li et al.* [2015] further showed that this future wetting trend is dominated by the thermodynamic contribution to the total mean moisture convergence. The 850 hPa winds regressions (arrows) show distinct differences for 20CR (Figures 1a and 1b), CMIP5 historical (Figures 1c and 1d), and RCP8.5 (Figures 1e and 1f) for both the monsoon region and the Pacific, which may have contributed to the discrepancies in the forced rainfall responses. These circulation changes are consistent with *Li et al.* [2015], who attributed the differences to the relative roles of aerosol and greenhouse gas (GHG) forcing during the historical period.

4. Summary

In this study, we have examined the ENSO-monsoon relationship for the 20th and 21st centuries using observations and CMIP5 model simulations. Running correlations between all-India rainfall and Niño 3.4 SST index show prominent decadal variability of the ENSO-monsoon relationship in observations. It is likely that the weakening in ENSO-monsoon relation in the recent decades is dominated by natural decadal variability rather than the global warming trend. The modeled ENSO-monsoon temporal correlation shows large intermodel spread, with the MMM significantly weaker than that for the observation. Although CMIP5 models tend to simulate well the ENSO-monsoon spatial structure when using the MMM, there is large uncertainty in the strength of the correlation within the model ensemble, ranging from slightly positive correlation in some models to strongly negative in others. In the RCP8.5 case, CMIP5 MMM shows a slightly weaker correlation than that in preindustrial and historical simulations, suggesting that the ENSO-monsoon relationship may change in the future.

We have applied S/N maximizing EOF analysis onto JJA seasonal averaged global SST of the CMIP5 ensemble to extract the externally forced signal and separated the anthropogenically forced component from the naturally varying component of ENSO variance. Results show that the natural component of the ENSO-monsoon relationship in the observed, CMIP5 historical, and the RCP8.5 scenario simulations are very similar in their spatial structure, indicating that the unforced ENSO-monsoon relationship is insensitive to the strength of the radiative forcing. When the radiative forced component is included, on the other hand, the ENSO-monsoon relationship in observations and CMIP5 historical simulations are relatively unchanged from the unforced component, but the RCP8.5 simulations show a slightly weaker negative relationship. The results suggest that natural variability is the dominant factor in determining the ENSO-monsoon relationship in observations and CMIP5 historical simulations. However in the 21st century, the wetting signal associated with SST warming may contribute to a weakening ENSO-monsoon relationship.

Our results have revealed that the negative ENSO-monsoon correlations are overall weak in CMIP5 MMM compared to observations and the variability among the models is rather large. Furthermore, there are large uncertainties in the forced rainfall response to SST warming during the historical period. It has been shown that GCMs have some difficulties in simulating and predicting regional monsoon variability and change, with aerosols being the major source of uncertainty [*Turner and Annamalai*, 2012; *Li et al.*, 2015]. Although it is noted that CMIP5 models are more skillful than CMIP3 models [*Sperber et al.*, 2013], there are still significant intermodel spreads [*Wang et al.*, 2014]. The ENSO-monsoon relationship could be a possible basis to evaluate the models and separate models into different categories for further mechanism-based studies. For example, if a model has a weak or opposite sign (positive) relationship between ENSO and Asian monsoon compared to observations, how would that difference affect the forced monsoon response to SST change? How would this type of models differ in their anthropogenically forced responses compared to the models that have

stronger (negative) ENSO-monsoon relationship? Further study will be conducted to study the mechanisms contributing to the differences in the models, as well as their possible implications for future monsoon change.

Acknowledgments
The authors acknowledge support from the National Oceanic and Atmospheric Administration Grants NOAA Award NA10OAR4310137 (Global Decadal Hydroclimate Variability and Change), the Office of Naval Research MURI grant 511 N00014-12-1-0911, and the Lamont Climate Center Award. We acknowledge the World Climate Research Programme's Working Group on Coupled Modeling and the climate modeling groups (listed in Table S1), for producing and making available the CMIP5 model output. Further information is available from the CMIP5 website (http://cmip-pcmdi.llnl.gov/cmip5/). We would like to thank Haibo Liu for downloading and preprocessing the CMIP5 data used in this study and Michela Biasutti, Yochanan Kushnir, and Tiffany Shaw for helpful discussions. We thank two anonymous reviewers for their helpful comments on the manuscript. LDEO Contribution 7891.

The Editor thanks two anonymous reviewers for their assistance in evaluating this paper.

References

Allen, M. R., and L. A. Smith (1997), Optimal filtering in singular spectrum analysis, *Phys. Lett.*, *234*(6), 419–428, doi:10.1016/S0375-9601(97)00559-8.

Annamalai, H., K. Hamilton, and K. R. Sperber (2007), The South Asian summer monsoon and its relationship with ENSO in the IPCC AR4 simulations, *J. Clim.*, *20*(6), 1071–1092, doi:10.1175/JCLI4035.1.

Ashrit, R. G., K. R. Kumar, and K. K. Kumar (2001), ENSO-monsoon relationships in a greenhouse warming scenario, *Geophys. Res. Lett.*, *28*(9), 1727–1730, doi:10.1029/2000GL012489.

Ashrit, R. G., H. Douville, and K. R. Kumar (2003), Response of the Indian monsoon and ENSO-monsoon teleconnection to enhanced greenhouse effect in the CNRM coupled model, *J. Meteorol. Soc. Jpn.*, *81*(4), 779–803, doi:10.2151/jmsj.81.779.

Ashrit, R. G., A. Kitoh, and S. Yukimoto (2005), Transient response of ENSO-monsoon teleconnection in MRI-CGCM2.2 climate change simulations, *J. Meteorol. Soc. Jpn.*, *83*(3), 273–291, doi:10.2151/jmsj.83.273.

Berkelhammer, M., A. Sinha, M. Mudelsee, H. Cheng, K. Yoshimura, and J. Biswas (2014), On the low-frequency component of the ENSO–Indian monsoon relationship: A paired proxy perspective, *Clim. Past*, *10*(2), 733–744, doi:10.5194/cp-10-733-2014.

Chang, C.-P., P. Harr, and J. Ju (2001), Possible roles of Atlantic circulations on the weakening Indian monsoon rainfall–ENSO relationship, *J. Clim.*, *14*(11), 2376–2380, doi:10.1175/1520-0442(2001)014<2376:PROACO>2.0.CO;2.

Chang, P., R. Saravanan, L. Ji, and G. C. Hegerl (2000), The effect of local sea surface temperatures on atmospheric circulation over the tropical Atlantic sector, *J. Clim.*, *13*(13), 2195–2216, doi:10.1175/1520-0442(2000)013<2195:TEOLSS>2.0.CO;2.

Chen, W., B. Dong, and R. Lu (2010), Impact of the Atlantic Ocean on the multidecadal fluctuation of El Niño–Southern Oscillation–South Asian monsoon relationship in a coupled general circulation model, *J. Geophys. Res.*, *115*, D17109, doi:10.1029/2009JD013596.

Chowdary, J. S., S.-P. Xie, H. Tokinaga, Y. M. Okumura, H. Kubota, N. Johnson, and X.-T. Zheng (2012), Interdecadal variations in ENSO teleconnection to the Indo-Western Pacific for 1870–2007, *J. Clim.*, *25*(5), 1722–1744, doi:10.1175/JCLI-D-11-00070.1.

Compo, G. P., et al. (2011), The twentieth century reanalysis project, *Q. J. R. Meteorol. Soc.*, *137*(654), 1–28, doi:10.1002/qj.776.

Cook, E. R., K. J. Anchukaitis, B. M. Buckley, R. D. D'Arrigo, G. C. Jacoby, and W. E. Wright (2010), Asian monsoon failure and megadrought during the last millennium, *Science*, *328*(5977), 486–489, doi:10.1126/science.1185188.

Gershunov, A., N. Schneider, and T. Barnett (2001), Low-frequency modulation of the ENSO–Indian monsoon rainfall relationship: Signal or noise?, *J. Clim.*, *14*(11), 2486–2492, doi:10.1175/1520-0442(2001)014<2486:LFMOTE>2.0.CO;2.

Harris, I., P. Jones, T. Osborn, and D. Lister (2014), Updated high-resolution grids of monthly climatic observations—The CRU TS3.10 dataset, *Int. J. Climatol.*, *34*(3), 623–642, doi:10.1002/joc.3711.

Hunt, B. (2014), The influence of stochasticism on Indian summer monsoon rainfall and its impact on prediction, *Clim. Dyn.*, *42*(9–10), 2271–2285, doi:10.1007/s00382-014-2119-3.

Ju, J., and J. Slingo (1995), The Asian summer monsoon and ENSO, *Q. J. R. Meteorol. Soc.*, *121*(525), 1133–1168, doi:10.1002/qj.49712152509.

Kelley, C., M. Ting, R. Seager, and Y. Kushnir (2012), The relative contributions of radiative forcing and internal climate variability to the late 20th century winter drying of the Mediterranean region, *Clim. Dyn.*, *38*(9–10), 2001–2015, doi:10.1007/s00382-011-1221-z.

Kinter, J. L., K. Miyakoda, and S. Yang (2002), Recent change in the connection from the Asian monsoon to ENSO, *J. Clim.*, *15*(10), 1203–1215, doi:10.1175/1520-0442(2002)015<1203:RCITCF>2.0.CO;2.

Kitoh, A. (2007), Variability of Indian monsoon-ENSO relationship in a 1000-year MRI-CGCM2.2 simulation, *Nat. Hazards*, *42*(2), 261–272, doi:10.1007/s11069-006-9092-z.

Kripalani, R., A. Kulkarni, S. Sabade, and M. Khandekar (2003), Indian monsoon variability in a global warming scenario, *Nat. Hazards*, *29*(2), 189–206, doi:10.1023/A:1023695326825.

Krishnamurthy, L., and V. Krishnamurthy (2014), Influence of PDO on South Asian summer monsoon and monsoon-ENSO relation, *Clim. Dyn.*, *42*(9–10), 2397–2410, doi:10.1007/s00382-013-1856-z.

Krishnamurthy, V., and B. N. Goswami (2000), Indian Monsoon–ENSO relationship on interdecadal timescale, *J. Clim.*, *13*(3), 579–595, doi:10.1175/1520-0442(2000)013<0579:IMEROI>2.0.CO;2.

Kumar, K. K., B. Rajagopalan, and M. A. Cane (1999), On the weakening relationship between the Indian monsoon and ENSO, *Science*, *284*(5423), 2156–2159, doi:10.1126/science.284.5423.2156.

Kumar, K. K., K. R. Kumar, R. G. Ashrit, N. R. Deshpande, and J. W. Hansen (2004), Climate impacts on Indian agriculture, *Int. J. Climatol.*, *24*(11), 1375–1393, doi:10.1002/joc.1081.

Kumar, K. K., B. Rajagopalan, M. Hoerling, G. Bates, and M. Cane (2006), Unraveling the mystery of Indian monsoon failure during El Niño, *Science*, *314*(5796), 115–119, doi:10.1126/science.1131152.

Lau, N.-C., and M. J. Nath (2000), Impact of ENSO on the variability of the Asian–Australian monsoons as simulated in GCM experiments, *J. Clim.*, *13*(24), 4287–4309, doi:10.1175/1520-0442(2000)013<4287:IOEOTV>2.0.CO;2.

Lau, N.-C., and B. Wang (2006), Interactions between the Asian monsoon and the El Niño/Southern Oscillation, in *The Asian Monsoon, Springer Praxis Books*, edited by B. Wang, pp. 479–512, Springer, Berlin.

Li, X., M. Ting, C. Li, and N. Henderson (2015), Mechanisms of Asian summer monsoon changes in response to anthropogenic forcing in CMIP5 models, *J. Clim.*, doi:10.1175/JCLI-D-14-00559.1, in press.

Mirza, M. M. Q. (2011), Climate change, flooding in South Asia and implications, *Reg. Environ. Change*, *11*(1), 95–107, doi:10.1007/s10113-010-0184-7.

Mishra, V., B. V. Smoliak, D. P. Lettenmaier, and J. M. Wallace (2012), A prominent pattern of year-to-year variability in Indian summer monsoon rainfall, *Proc. Natl. Acad. Sci.*, *109*(19), 7213–7217, doi:10.1073/pnas.1119150109.

Rasmusson, E. M., and T. H. Carpenter (1983), The relationship between eastern equatorial Pacific sea surface temperatures and rainfall over India and Sri Lanka, *Mon. Weather Rev.*, *111*(3), 517–528, doi:10.1175/1520-0493(1983)111<0517:TRBEEP>2.0.CO;2.

Ropelewski, C. F., and M. S. Halpert (1987), Global and regional scale precipitation patterns associated with the El Niño/Southern Oscillation, *Mon. Weather Rev.*, *115*(8), 1606–1626, doi:10.1175/1520-0493(1987)115<1606:GARSPP>2.0.CO;2.

Smith, T. M., R. W. Reynolds, T. C. Peterson, and J. Lawrimore (2008), Improvements to NOAA's historical merged land-ocean surface temperature analysis (1880–2006), *J. Clim.*, *21*(10), 2283–2296, doi:10.1175/2007JCLI2100.1.

Sperber, K., H. Annamalai, I.-S. Kang, A. Kitoh, A. Moise, A. Turner, B. Wang, and T. Zhou (2013), The Asian summer monsoon: An intercomparison of CMIP5 vs. CMIP3 simulations of the late 20th century, *Clim. Dyn.*, *41*(9–10), 2711–2744, doi:10.1007/s00382-012-1607-6.

Taschetto, A. S., A. S. Gupta, N. C. Jourdain, A. Santoso, C. C. Ummenhofer, and M. H. England (2014), Cold tongue and warm pool ENSO events in CMIP5: Mean state and future projections, *J. Clim.*, *27*(8), 2861–2885, doi:10.1175/JCLI-D-13-00437.1.

Taylor, K. E., R. J. Stouffer, and G. A. Meehl (2012), An overview of CMIP5 and the experiment design, *Bull. Am. Meteorol. Soc.*, *93*(4), 485–498, doi:10.1175/BAMS-D-11-00094.1.

Ting, M., Y. Kushnir, R. Seager, and C. Li (2009), Forced and internal twentieth-century SST trends in the North Atlantic, *J. Clim.*, *22*(6), 1469–1481, doi:10.1175/2008JCLI2561.1.

Ting, M., Y. Kushnir, R. Seager, and C. Li (2011), Robust features of Atlantic multi-decadal variability and its climate impacts, *Geophys. Res. Lett.*, *38*, L17705, doi:10.1029/2011GL048712.

Torrence, C., and P. J. Webster (1999), Interdecadal changes in the ENSO–monsoon system, *J. Clim.*, *12*(8), 2679–2690, doi:10.1175/1520-0442(1999)012<2679:ICITEM>2.0.CO;2.

Trenberth, K. E. (1997), The definition of El Niño, *Bull. Am. Meteorol. Soc.*, *78*(12), 2771–2777, doi:10.1175/1520-0477(1997)078<2771:TDOENO>2.0.CO;2.

Turner, A. G., and H. Annamalai (2012), Climate change and the South Asian summer monsoon, *Nat. Clim. Change*, *2*(8), 587–595, doi:10.1038/nclimate1495.

Venzke, S., M. R. Allen, R. T. Sutton, and D. P. Rowell (1999), The atmospheric response over the North Atlantic to decadal changes in sea surface temperature, *J. Clim.*, *12*(8), 2562–2584, doi:10.1175/1520-0442(1999)012<2562:TAROTN>2.0.CO;2.

Wang, B., R. Wu, and T. Li (2003), Atmosphere–warm ocean interaction and its impacts on Asian–Australian monsoon variation, *J. Clim.*, *16*(8), 1195–1211, doi:10.1175/1520-0442(2003)16<1195:AOIAII>2.0.CO;2.

Wang, B., S.-Y. Yim, J.-Y. Lee, J. Liu, and K.-J. Ha (2014), Future change of Asian-Australian monsoon under RCP 4.5 anthropogenic warming scenario, *Clim. Dyn.*, *42*(1–2), 83–100, doi:10.1007/s00382-013-1769-x.

Webster, P. J., and S. Yang (1992), Monsoon and ENSO: Selectively interactive systems, *Q. J. R. Meteorol. Soc.*, *118*(507), 877–926, doi:10.1002/qj.49711850705.